HHS Public Access

Author manuscript

Kidney Int. Author manuscript; available in PMC 2013 January 01.

Published in final edited form as:

Kidney Int. 2012 July ; 82(2): 172–183. doi:10.1038/ki.2012.20.

Targeted proximal tubule injury triggers interstitial fibrosis and glomerulosclerosis

Ivica Grgic, MD[1,3,6], **Gabriela Campanholle, PhD**[1,6], **Vanesa Bijol, MD**[2], **Chang Wang, MD**[1], **Venkata S. Sabbisetti, PhD**[1], **Takaharu Ichimura, PhD**[1], **Benjamin D. Humphreys, MD, PhD**[1,4], and **Joseph V. Bonventre, MD, PhD**[1,5]

[1]Renal Division, Department of Medicine, Brigham and Women's Hospital, Harvard Medical School, Boston, Massachusetts

[2]Department of Pathology and Laboratory Medicine, Brigham and Women's Hospital, Harvard Medical School, Boston, Massachusetts

[3]Department of Internal Medicine and Nephrology, Philipps-University, Marburg, Germany

[4]Harvard Stem Cell Institute, Cambridge, Massachusetts

[5]Harvard-Massachusetts Institute of Technology, Division of Health Sciences and Technology, Cambridge, Massachusetts

Abstract

Chronic kidney disease (CKD) remains one of the leading causes of death in the developed world and acute kidney injury (AKI) is now recognized as a major risk factor in its development. Understanding the factors leading to CKD after acute injury are limited by current animal models of AKI which concurrently target various kidney cell types such as epithelial, endothelial and inflammatory cells. Here we developed a mouse model of kidney injury using the Six2-Cre-LoxP technology to selectively activate expression of the simian diphtheria toxin receptor in renal epithelia derived from the metanephric mesenchyme. By adjusting the timing and dose of diphtheria toxin a highly selective model of tubular injury was created to define the acute and chronic consequences of isolated epithelial injury. The diphtheria toxin-induced sublethal tubular epithelial injury was confined to the S1 and S2 segments of the proximal tubule rather than being widespread in the metanephric mesenchyme derived epithelial lineage. Acute injury was promptly followed by inflammatory cell infiltration and robust tubular cell proliferation leading to complete recovery after a single toxin insult. In striking contrast, three insults to renal epithelial cells at one week intervals resulted in maladaptive repair with interstitial capillary loss, fibrosis and glomerulosclerosis which was highly correlated with the degree of interstitial fibrosis. Thus,

Correspondence: Ivica Grgic MD (igrgic@rics.bwh.harvard.edu), Joseph V. Bonventre MD, PhD (joseph_bonventre@hms.harvard.edu), Brigham and Women's Hospital, 75 Francis Street, Boston, MA 02115, phone: 617-732-6020, fax: 617-582-6010.

[6]These authors contributed equally to this work.

Disclosures

J.V.B. is co-inventor on KIM-1 patents assigned to Partners Healthcare and licensed to BiogenIdec, J and J, Sekisui and a number of research reagent companies.

selective epithelial injury can drive the formation of interstitial fibrosis, capillary rarefaction and potentially glomerulosclerosis, substantiating a direct role for damaged tubule epithelium in the pathogenesis of CKD.

Introduction

Acute kidney injury (AKI) is a very common clinical syndrome, frequently progressing to kidney failure and associated with increased cost, length of hospital stay and adverse short and long term outcomes with accelerated progression of chronic kidney disease [1–5]. The molecular mechanisms linking AKI to CKD remain obscure.

AKI is a complex disease entity involving tubular epithelial, endothelial and inflammatory cells. Understanding the pathophysiology of AKI and its sequelae requires dissection of the relative contributions of these different cell types to the origination and course of the disease. Such knowledge will stimulate and guide efforts to develop new therapeutic approaches.

Studying the biological properties of individual cell types in AKI is complicated by two major obstacles: the kidney is a highly heterogeneous organ with more than two dozen different cell types; and commonly used rodent AKI models such as ischemia-reperfusion (IR) or toxic injury involve primary damage to multiple cell types including the endothelium and tubular epithelium [6]. Damage in these models is associated with processes that operate concurrently making it difficult to determine the relative importance of primary injury to a particular cell type in the context of disease progression.

One strategy to overcome the limitations of current AKI models is to restrict the primary injury to one specific cell type. We devised and characterized a new model of selective renal epithelial injury by applying *Cre-LoxP* technology in combination with *toxin receptor mediated cell knockout* (TRECK) [7]. We target epithelial cells for two reasons: first, tubular epithelial cells are generally known to exhibit a pronounced susceptibility to kidney insults showing the most overt signs of damage and regeneration after injury, and second, a growing body of evidence implicates a key signaling role of dedifferentiated epithelial cells in the initiation and progression of renal fibrosis [4]. We used this model to address the following questions: (i) Does isolated renal epithelial injury/repair remain self-contained within the tubular compartment or does it affect other non-epithelial cell systems, possibly through activation of the immune system? (ii) How is the regenerative response of the renal epithelium affected after targeted disruption and is there a difference in long-term outcome between single and multiple “hits”? (iii) If maladaptive repair occurs, does it manifest with typical features of tubulointerstitial fibrosis, lead to capillary rarefaction and potentially affect the glomerulus?

Results

Bigenic DTR^{rec} mice show kidney-specific induction of simian diphtheria toxin receptor expression

To obtain a system of epithelial cell-specific injury in the kidney we crossed the Six2-GFPCre mouse [8] with a Cre-inducible diphtheria toxin receptor (iDTR) transgenic mouse [9], generating bigenic Six2-GFPCre^{+};iDTR^{+} mice - hereafter referred to as DTR^{rec} (DTR$^{renal\ epithelial\ cell}$) mice - at the expected mendelian ratio (Fig.S1a). The transcription factor Six2 is transiently expressed during the developmental period of active nephrogenesis in the cap mesenchyme which gives rise to all nephron cell types derived from the metanephric mesenchyme, including podocytes, proximal tubules, loop of Henle and distal tubules [8]. The collecting duct system, by contrast, originates from a different embryological source, the ureteric bud. In this model, the Six2 promoter drives a GFP-tagged Cre recombinase which mediates excision of the *loxP*-flanked STOP cassette located between the *Gt(ROSA)26Sor* locus and the open reading frame of the simian DTR in renal epithelial precursors only (Fig.1A). As a result, this recombination induces constitutive and heritable DTR expression in all mesenchyme-derived renal epithelial cells, from Bowman's capsule to the junction of connecting tubule and collecting duct (Fig.S1b). RT-PCR analysis confirmed high expression levels of DTR in kidney but not in other tested organs of DTR^{rec} mice (Fig.1B). DTR expression during embryogenesis had no impact on kidney development or animal growth. The number of glomeruli, kidney architecture and body weight were comparable in DTR^{rec} mice and littermate controls (Fig.S1c&d).

DT triggers acute kidney injury in DTR^{rec} mice

DTR^{rec} animals exposed to 0.25–50μg/kg DT showed a progressive rise in serum creatinine and succumbed to kidney failure within one week after injection (Fig.1C&D). Microscopic examination revealed diffuse acute tubular injury with extensive degenerative changes of epithelial cells and accumulation of cellular debris in the lumen (Fig.1E). Abnormalities were most prominent in epithelial cells at the glomerulotubular junction and S1 and S2 segments of proximal tubules but were also noted in more distal nephron segments, including distal tubules. Collecting ducts were uninjured, consistent with their origin from the ureteric bud rendering them non-susceptible to DT in this model. Also, glomerular tufts (80–120 routinely examined per section) and vasculature were unaffected (Fig.S2). The absence of podocyte injury was unexpected, since DTR was predicted to be expressed in podocytes. Gross examination of other organs after DT administration revealed no abnormalities. Higher doses of DT proved consistently lethal and thus unsuitable for the study of repair processes and long-term effects. A series of titration experiments were conducted to determine the sublethal toxin dose-response in our model (Fig.1C&D). This sublethal DT dose (0.15μg/kg) was then used for all subsequent experiments of tubular cell injury.

Sublethal doses of DT damage nephron segments S1/S2 in DTR^{rec} mice

Renal tissue was evaluated at various time points after sublethal doses of DT and signs of acute tubular injury were found to be most prominent at day 3. Damage was limited to early proximal tubular segments S1 and S2 of the kidney cortex (Fig.2&3; Fig.S3). There was loss

of brush borders, luminal distension, nuclear condensation and karyorrhectic debris. Some nephrons showed regenerative nuclear changes with isolated mitotic figures. Electron microscopic examination of glomeruli (7–10 per animal) demonstrated normal ultrastructural features of podocytes including absence of podocyte foot process effacement (Fig.2C–E; Fig.S4a). The glomerular basement membranes were of normal thickness and texture, endothelial cells had regular fenestrae and the mesangium was of normal cellularity and structure. By contrast, proximal tubular cell abnormalities were readily identifiable and widespread on the same specimen and included degeneration of cytoplasmic organelles and nuclei with karyopyknosis and karyorrhexis, and decomposition and breakage of cell membranes (Fig.2F–H). No damage was observed in collecting ducts (Fig.2F). These morphological changes were paralleled by enhanced TUNEL staining of fragmented DNA indicating induction of tubular apoptosis predominantly in the cortex (Fig.3A–D). Segment specific analysis revealed that the vast majority of $TUNEL^+$ epithelial cells was located in LTA^+ proximal tubules (95.2 ± 0.8%). No TUNEL+ cells were observed in glomerular tufts or DBA^+ collecting ducts (Fig.3E–G; Fig.S3). Morphological examination of THP/uromodulin$^+$ thick ascending limbs (TAL) which are located between proximal tubule and collecting duct showed that sublethal doses of DT did not affect this intermediate portion of the nephron whereas lethal doses clearly did (Fig.3H–J). Kidney injury molecule 1 (Kim-1) [10] protein was induced in a time dependent manner subsequent to DT exposure in proximal tubule cells including those at the glomerulotubular junction (Fig.S4b). Urinary Kim-1 was also markedly increased (Fig.3K). By contrast, urinary NGAL, another marker of kidney injury but known to be produced by injured distal tubules [11], was essentially unchanged (Fig.3L), supporting the notion that injury was significantly less or absent in distal tubules with sublethal doses of DT. While serum creatinine levels were not significantly changed, analysis of the urinary protein composition showed a transient increase in urinary excretion of proteins >50kDa (Fig.3M; Fig.S4c–e).

Epithelial injury to segments S1/S2 is sufficient to trigger inflammatory response

All three major inflammatory cell types, namely macrophages ($F4/80^+$), T cells ($CD3^+$) and neutrophils, showed a focal, mild to moderate increase in cell numbers in the tubulointerstitium of DT-injured kidneys (Fig.4A–C). Also, leukocyte esterase activity was increased in the urine of DTR^{rec} mice after DT exposure (Fig.4D). In DT-injured kidney tissue we found a 2.5-fold (day 1) and 14-fold (day 3) upregulation of ICAM-1, an intercellular adhesion molecule expressed, although not exclusively, in membranes of endothelial cells and instrumental for leukocyte transmigration, which may suggest secondary activation of adjacent endothelium (Fig.4E).

Effective regenerative response after single injury to renal epithelium

At day 1, 3 and 7 after DT (0.15μg/kg) 2.4 ± 0.14% ($p<0.01$ vs. uninjured control [0.9 ± 0.12%]), 13.0 ± 3.12% ($p<0.05$) and 13.1 ± 0.95% ($p<0.001$), respectively, of all tubular cells stained positive for Ki67 indicating a pronounced proliferative response (Fig.5A). To study proliferative activity longitudinally we pulse-labeled proliferating cells by daily intraperitoneal injections of BrdU (50μg/g). By day 3 after DT-induced injury at least 12.3 ± 3.2% ($p<0.05$ vs. uninjured control [0.8 ± 0.1%]) of all tubular epithelial cells had incorporated BrdU (Fig.5B). By day 7, this fraction had further risen to 30.1 ± 4.8% ($p<0.01$

vs. control [2.1 ± 0.5%]). Segment specific analysis revealed that the majority of proliferating renal epithelial cells were located in LTA^+ proximal tubules of the cortex (88.1 ± 2.5%) and only sporadically found in glomerular tufts or DBA^+ collecting ducts (Fig.5C–E; Fig.S5). In sublethally injured DTR^{rec} kidneys the general prevalence of $Ki67^+$ epithelial cells was significantly higher in cortex compared to medulla. Of note, in lethally injured kidneys this ratio was reversed, reflecting not only involvement of more distal parts of the nephron with higher doses of DT, but also the increased severity of damage to proximal tubules with fewer surviving cells left to participate in the reparative response (Fig.5F–H). Examination of kidneys from DTR^{rec} mice at 5 weeks after one-time treatment with DT showed normal renal histology without residual evidence of damage or scarring indicating complete recovery from acute, non-recurring injury to the renal epithelium.

Repeatedly injured renal epithelium triggers fibrogenesis

To study the long-term outcomes of targeted renal epithelial injury DTR^{rec} mice were divided into three groups: one group received a single sublethal dose of DT (0.15μg/kg), the other two groups received three injections of either DT (0.15μg/kg) or vehicle (PBS) alone at weekly intervals. Kidneys were harvested at 5 weeks for analyses. Histopathological examination revealed no abnormalities in kidneys of vehicle-treated or single dose DT-injected animals. By contrast, all three dose DT-treated DTR^{rec} mice exhibited chronic tubulointerstitial damage with varying degrees of tubular atrophy and interstitial fibrosis (Fig.6A). Atrophic tubules showed flat and very simplified epithelial lining with thickened and wrinkled tubular basement membranes, frequently containing hyaline casts. Areas of tubular atrophy were associated with interstitial fibrosis and chronic inflammatory infiltrates and kidneys with advanced tubulointerstitial scarring additionally showed focal global and segmental glomerulosclerosis, generally involving less than 25% of all glomeruli. There was a strong positive correlation between the extent of interstitial fibrosis/tubular atrophy and the number of sclerosed glomeruli and degree of albuminuria, respectively (Fig.6B&C). Animals with advanced tubulointerstitial damage also exhibited elevated serum creatinine levels indicating significantly compromised renal function (0.6 ± 0.1 mg/dL vs. ctrl 0.18 ± 0.02 mg/dL). Moreover, RT-PCR analyses demonstrated significantly increased kidney expression of key profibrotic cytokine TGFβ1 and major matrix components (collagen1α1, fibronectin) (Fig.6D). Consistent with RT-PCR results, we detected distinct ECM deposits in the tubulointerstitial space of repeatedly injured DTR^{rec} kidneys by Masson-Trichrome staining (Fig.6E). Kim-1 protein levels were elevated in both kidney sections and urine of animals injected thrice with DT when compared to controls (Fig.6F&G).

Ki67-staining revealed that a substantial fraction of interstitial but also tubular epithelial cells exhibited proliferative activity in diseased kidneys (Fig.S6a). There was a dramatic increase in the number of pericytes/perivascular fibroblasts (PDGF receptor β^+), myofibroblasts (αSMA^+), *fibroblast specific protein-1* expressing cells ($FSP\text{-}1/S100A4^+$) as well as macrophages ($F4/80^+$) in DTR^{rec} kidneys after repeated DT injury (Fig.7A&B; Fig.S6b&c). By contrast, the number of endothelial cells ($CD31/PECAM^+$) was significantly reduced in these kidneys indicating capillary drop out (Fig.7C). Thus, repeated targeted injury to the renal epithelium leads to tubulointerstitial fibrosis, endothelial cell rarefaction and glomerulosclerosis.

Discussion

Despite evidence of a possible causative clinical connection between AKI and the subsequent development of CKD, the characteristics of the specific cellular contributions to the pathophysiology of fibrosis remain unclear. By generating bigenic Six2-GFPCre^{+};iDTR^{+} (DTR^{rec}) mice we were able to permanently render renal epithelial cells susceptible to DT. Simian DT receptor expression in this model was organ-specific and robust. By using lower, sublethal doses of DT we were able to limit injury to the early proximal tubular segments S1 and S2. This phenomenon may be explained by the pharmacokinetics of DT which can cross the rodent glomerular barrier into the urinary space, thus exposing the proximal tubular epithelium to the highest toxin concentrations. The high water reabsorption rate in these segments may lead to an increase in local DT levels. DT molecules that have bound to DT receptors are internalized and hence removed from the urinary space and can therefore not affect more distal parts of the nephron. With higher doses of DT this specificity is increasingly lost. Of note, despite marked damage to proximal tubular epithelium, careful light microscopic analyses as well as electron microscopy revealed no detectable abnormalities of glomerular tufts in general and the visceral epithelium (podocytes) in particular. This finding was surprising since we in fact expected podocytes to express the DT receptor and thus also be rendered susceptible to DT exposure. Reasons for the absence of podocyte injury in this model may include an insufficient deletion frequency of the STOP cassette in some progenitor cells, a lower expression strength of the *Gt(ROSA)26Sor* promoter in podocytes compared to tubules, poor cell-surface expression of DT receptor in murine podocytes and/or a lower overall susceptibility to DT in murine podocytes as compared to renal tubular cells. Interestingly, this feature appears not be restricted to podocytes only as Buch *et al.* have reported other resistant cell types in their original description of the iDTR mouse for reasons unknown [9]. Conversely, the relatively high susceptibility of proximal tubules may in part be accounted for by local DT elevations due to prominent water abstraction in these segments. Although the Six2-GFPCre driver has, in our hands, proven to be highly efficient and consistent in labeling mesenchyme-derived renal epithelial cells in a number of different floxed reporter mice [12], we cannot completely rule out the possibility of mosaicism in DTR expression in this particular bigenic mouse model. Regardless of the reason for the absence of podocyte injury, a single sublethal DT bolus was sufficient to induce a substantial apoptotic reaction in the early proximal tubule. This mechanism of cell death differs fundamentally from that of another recently reported epithelial specific injury model in which tubular overproduction of TGFβ1 was shown to cause cellular demise by autophagy and not by apoptosis [13]. Administration of sublethal DT doses resulted in subclinical AKI with continued urine output and transient albuminuria which is common in tubular injury and reflects the reduced reabsorptive capacity of dysfunctional proximal epithelium.

Inflammation is a well known feature of AKI [14, 15]. Our data reveal that targeted injury to the renal epithelium is sufficient to trigger a mild to moderate inflammatory response with attraction of inflammatory cells. What exact signaling mechanisms underlie this activation warrants further exploration. As recent data suggest, one of these mechanisms may include

the *toll-like receptor* (TLR) signaling system [16, 17], which responds to *damage associated molecular pattern molecules* (DAMPs) that dying epithelial cells release [18].

Tubular regeneration after single, DT-induced injury to renal epithelium in this model was robust and efficient, leading to a complete restoration of kidney architecture without evidence of prior damage. By contrast, three doses of DT resulted in maladaptive repair and manifested as tubulointerstitial fibrosis and tubular atrophy. Thus, the cumulative effects of repetitive episodes of subclinical AKI lead to progressive tubulointerstitial fibrosis characteristic of CKD. There are a number of possible explanations for this. First, recurrent injury may lead to premature cell senescence as the replicative capacity of epithelial cells is exhausted after repeated impairment. Second, repeatedly injured tubular cells may remain in a dedifferentiated state even after repopulation of the tubules is complete. Dedifferentiated tubules are believed to produce a myriad of bioactive molecules with autocrine and paracrine functions which regulate the immediate repair process following acute injury, but may have detrimental effects in the long run if not reversed [19–21]. For instance, in models of CKD a persistent expression of platelet-derived growth factor B-chain (PDGF-B) was observed in dedifferentiated tubular cells, but not in tubules with a differentiated phenotype [20, 21]. Interestingly, cells expressing the PDGF receptor β, an accepted marker of pericytes and perivascular fibroblasts [22, 23], were found enriched in the tubulointerstitium surrounding these tubules, suggesting a possible paracrine ligand-receptor coupling – a model consistent with recent findings showing that myofibroblast progenitors reside in the interstitium adjacent to epithelia [24]. De Borst *et al*. reported that c-Jun NH_2-terminal kinase (JNK) remained active in proximal tubule cells for weeks after ischemic insult and was associated with tubulointerstitial inflammation and fibrosis [25]. Our laboratory found a direct connection between JNK signaling and the upregulation of profibrotic cytokines such as TGFβ1 and CTGF in proximal tubule epithelium using ischemic, toxic and obstructive models of kidney injury [4]. Cell cycle arrest in G2/M activated JNK in these cells and resulted in a fibrotic outcome that was reduced with JNK inhibition. The persistence of PDGF-B expression and JNK activity likely represent only two in a variety of yet unidentified profibrotic and phlogistic factors emitted by proximal tubules that fail to differentiate or are delayed in the process. Finally, capillary loss was observed in DTR^{rec} kidneys following repeated epithelial injury. Activation and migration of PDGFRβ+ pericytes in injured kidney may disrupt the endothelium-pericyte crosstalk hereby contributing to capillary rarefaction, progressive ischemia and aggravation of tubulointerstitial damage [22, 26].

Our findings also show that repeated DT-induced injury to renal epithelium may affect glomerular anatomy and function in the long term. There was a strong correlation between the degree of tubulointerstitial fibrosis/ tubular atrophy and the number of globally or segmentally sclerosed glomeruli. No glomerulosclerosis was detected in cases with mild tubulointerstitial fibrosis. Since our histological data suggest that the site of primary injury did not include cells of the glomerular tuft, we speculate that glomerular pathology occurred secondary to repeated DT-mediated acute tubular injury in this model. One reason for this may be the increasing loss of capillaries observed in tubulointerstitial fibrosis, leading to a progressive reduction of glomerular blood flow. In addition, the close proximity of early

proximal tubular segments to the glomerular tuft and their *per continuum* connection via the urinary space could result in paracrine signaling from injured and regenerating/undifferentiated epithelium to directly impact the glomerulus [27]. Alternatively, a progressive tubulointerstitial reaction originating around atrophic and undifferentiated tubules may directly encroach upon the glomerular tuft. Ultimately, the glomerulotubular junction may, in some nephrons, become progressively narrowed and disconnect the tubule from the upstream glomerulus [28].

In summary, we have developed a new, more targeted model of acute renal injury to study pathophysiological mechanisms and outcomes in the kidney after isolated disruption of renal epithelial cells. We show that injured proximal tubule epithelium is capable of triggering an inflammatory response and that it can effectively regenerate. Repeated injury resulted in maladaptive repair, giving rise to tubulointerstitial fibrosis, tubular atrophy and potentially secondary glomerulosclerosis. Thus, acute injury to proximal segments of the tubule was sufficient to produce the full spectrum of pathological changes associated with progressive CKD in this model. Interventions aimed at proximal signaling events originating from tubules may prevent pathological cascades that lead to CKD.

Materials and Methods

Mouse maintenance and experiments

All mice were maintained in barrier according to institutional guidelines. Six2-GFP-Cre transgenic mice (129/B6) were crossed with iDTR mice (C57BL/6) to obtain bigenic offspring (DTR^{rec}). Genomic DNA was obtained from tail biopsies and genotyping performed using the following primers: for iDTR (wt product ~620 bp, iDTR product ~240 bp) 5’-aaagtcgctctgagttgttat-3’ (RosaFA), 5’-ggagcgggagaaatggatatg-3’ (RosaRA) and 5’-catcaaggaaaccctggactactg-3’ (SpliAcB); for Cre (~410 bp) 5’-ctaatcgccatcttccagcagg-3’ (F), 5’-aggtgtagagaaggcacttagc-3’ (R). For renal epithelial injury DTR^{rec} mice were injected intraperitoneally with variable doses of diphtheria toxin as indicated. In some experiments, BrdU was administered daily at 50μg/g in 0.9% saline. Blood samples were collected by tail vein or cardiac puncture and mice placed in metabolic cages for urine collection prior to and at various time points after DT injection.

Tissue preparation and histology

Mice were sacrificed under deep anesthesia and immediately perfused via left ventricle with ice-cold PBS for 1 min. Kidneys were removed, cut sagitally and fixed either in 4% PLP (1–2 hr) followed by cryoprotection in 30% sucrose (overnight) and snap-freezing in OCT (Sakura FineTek) for cryosectioning or in 10% neutral buffered formalin for paraffin-embedding. Histological analysis was performed on paraffin-embedded and serially cut kidney sections (3μm) stained with hematoxylin and eosin (H&E), periodic acid-Schiff (PAS), and Masson’s trichrome. Analysis of acute tubular injury included the evaluation of the severity of injury and the distribution of acute tubular damage. The degree of injury was scored semiquantitatively on a 0 to 4 scale (0, no lesion; 1, minimal (minor focal changes); 2, mild (mild nuclear condensation, karyorrhexis, and brush border loss); 3, moderate (pronounced changes with prominent karyorrhexis, degeneration of cytoplasm, single cell

necrosis, and cellular debris in the tubular lumen); 4, severe (severe degenerative changes with distinct tubular dilatation, sloughing of the epithelial layer, and denudation of tubular basement membrane). The distribution was graded as focal if ≤ 49% and diffuse if ≥ 50% of the cortex showed acute tubular changes. Semiquantitative analysis of chronic damage included the estimation of cortical tubular atrophy and interstitial fibrosis, and was graded as minimal (involving < 5% of cortex), mild (5–24%), moderate (25–49%), and severe (≥ 50%). For assessment of glomerular involvement, an average of 80–120 glomeruli per section were examined on multiple levels. All scoring was performed in a blinded manner.

Electron microscopy

Portions of kidneys were fixed in Karnovsky's fixative and processed for electron microscopic studies by standard procedures. Semithin sections of each block were stained with toluidine-blue stain and examined by light microscopy to select for ultrathin sectioning. Ultrathin sections were stained with uranyl acetate and lead citrate and examined by electron microscopy.

Renal function

Plasma and urine creatinine concentrations were determined by the picric acid method. Qualitative and quantitative urine protein analysis was performed by chip-based capillary electrophoresis using the Agilent 2100 Bioanalyzer System (Agilent Technologies) and by Multistix 8 SG Urinalysis Strips (Siemens).

RT-PCR

RNA was extracted from snap-frozen tissue stored at −80°C using standard techniques (TRIzol, Sigma). Reverse transcription was performed with the M-MLV reverse transcriptase kit (Promega) producing cDNA. Real-time PCR was performed using the iQ-SYBR Green supermix (BioRad) and the iQ5 Multicolor Real-Time PCR Detection System (BioRad) for detection of mRNA levels of *Hbegf (simian DTR), Icam-1, Tgfb1, Col1a1 and Fn1 (fibronectin)*. Housekeeping gene *18S* was used as the internal control.

Microbead-based immunoassay

Urine Kim-1 and NGAL protein concentrations were measured using Luminex xMAP technology as previously described [29]. For additional information see Supplement.

Immunofluorescence staining

Immunohistological staining of kidney sections was performed as previously described [4]. Briefly, sections were labeled with primary and corresponding FITC- or Cy3-conjugated secondary antibodies (Jackson ImmunoResearch), and mounted with DAPI-containing Vectashield mounting medium (Vector Labs). Staining was examined by fluorescence microscopy (Nikon C1 confocal and Nikon eclipse 90i). For additional information see Supplement.

Analysis of apoptosis

Cell apoptosis was detected on paraffin sections by *in situ* TdT-mediated dUTP-biotin nick end labeling (TUNEL) according to the standard protocol (Roche) followed by DAPI nuclear counterstaining. The prevalence of apoptosis was expressed as the ratio of TUNEL-positive renal tubular cells to total renal tubular cell nuclei ($DAPI^+$).

Statistics

Data are given as mean ± SEM. Statistical analysis was performed using the unpaired Student's *t* test to determine differences between two groups and analysis of variance to compare data among groups. Kaplan-Meier curves were compared by the *log-rank test for trend* and the *Mantel-Cox test*, dependence between variables assessed by Spearman's rho. P values of less than 0.05 were considered statistically significant.

Supplementary Material

Refer to Web version on PubMed Central for supplementary material.

Acknowledgements

I.G. was supported by a fellowship from the Deutsche Forschungsgemeinschaft (GR 3301/4-1) and grants from the German Kidney Foundation, German Society of Hypertension and University Medical Center Giessen and Marburg. G.C. was supported by a grant from FAPESP (06/06236-2) and CAPES. This work was supported by US National Institutes of Health (NIH) grants DK88923 and DK84316 to B.D.H and DK72381 and DK39773 to J.V.B. The authors wish to thank Dr. Akio Kobayashi and Dr. Andrew P. McMahon for the gift of the Six2-GFPCre mouse, Dr. Ari Waisman for the gift of the iDTR mouse, and Eileen O'Leary for assistance in mouse colony maintenance.

Sources of support: Deutsche Forschungsgemeinschaft, US National Institutes of Health (NIH)

References

1. Thadhani R, Pascual M, Bonventre JV. Acute renal failure. N Engl J Med. 1996; 334:1448–1460. [PubMed: 8618585]
2. Chertow GM, Burdick E, Honour M, et al. Acute kidney injury, mortality, length of stay, and costs in hospitalized patients. J Am Soc Nephrol. 2005; 16:3365–3370. [PubMed: 16177006]
3. Hsu CY. Where is the epidemic in kidney disease? J Am Soc Nephrol. 2010; 21:1607–1611. [PubMed: 20813868]
4. Yang L, Besschetnova TY, Brooks CR, et al. Epithelial cell cycle arrest in G2/M mediates kidney fibrosis after injury. Nat Med. 2010; 16:535–543. 531p following 143. [PubMed: 20436483]
5. Okusa MD, Chertow GM, Portilla D. The nexus of acute kidney injury, chronic kidney disease, and World Kidney Day 2009. Clin J Am Soc Nephrol. 2009; 4:520–522. [PubMed: 19225036]
6. Heyman SN, Lieberthal W, Rogiers P, et al. Animal models of acute tubular necrosis. Curr Opin Crit Care. 2002; 8:526–534. [PubMed: 12454537]
7. Saito M, Iwawaki T, Taya C, et al. Diphtheria toxin receptor-mediated conditional and targeted cell ablation in transgenic mice. Nat Biotechnol. 2001; 19:746–750. [PubMed: 11479567]
8. Kobayashi A, Valerius MT, Mugford JW, et al. Six2 defines and regulates a multipotent self-renewing nephron progenitor population throughout mammalian kidney development. Cell Stem Cell. 2008; 3:169–181. [PubMed: 18682239]
9. Buch T, Heppner FL, Tertilt C, et al. A Cre-inducible diphtheria toxin receptor mediates cell lineage ablation after toxin administration. Nat Methods. 2005; 2:419–426. [PubMed: 15908920]
10. Han WK, Bonventre JV. Biologic markers for the early detection of acute kidney injury. Curr Opin Crit Care. 2004; 10:476–482. [PubMed: 15616389]

11. Paragas N, Qiu A, Zhang Q, et al. The Ngal reporter mouse detects the response of the kidney to injury in real time. Nat Med. 2011; 17:216–222. [PubMed: 21240264]
12. Humphreys BD, Valerius MT, Kobayashi A, et al. Intrinsic epithelial cells repair the kidney after injury. Cell Stem Cell. 2008; 2:284–291. [PubMed: 18371453]
13. Koesters R, Kaissling B, Lehir M, et al. Tubular overexpression of transforming growth factor-beta1 induces autophagy and fibrosis but not mesenchymal transition of renal epithelial cells. Am J Pathol. 2010; 177:632–643. [PubMed: 20616344]
14. Bonventre JV, Zuk A. Ischemic acute renal failure: an inflammatory disease? Kidney Int. 2004; 66:480–485. [PubMed: 15253693]
15. Jang HR, Rabb H. The innate immune response in ischemic acute kidney injury. Clin Immunol. 2009; 130:41–50. [PubMed: 18922742]
16. Wu H, Chen G, Wyburn KR, et al. TLR4 activation mediates kidney ischemia/reperfusion injury. J Clin Invest. 2007; 117:2847–2859. [PubMed: 17853945]
17. Leemans JC, Stokman G, Claessen N, et al. Renal-associated TLR2 mediates ischemia/reperfusion injury in the kidney. J Clin Invest. 2005; 115:2894–2903. [PubMed: 16167081]
18. Wu H, Ma J, Wang P, et al. HMGB1 contributes to kidney ischemia reperfusion injury. J Am Soc Nephrol. 2010; 21:1878–1890. [PubMed: 20847143]
19. Venkatachalam MA, Griffin KA, Lan R, et al. Acute kidney injury: a springboard for progression in chronic kidney disease. Am J Physiol Renal Physiol. 2010
20. Suzuki T, Kimura M, Asano M, et al. Role of atrophic tubules in development of interstitial fibrosis in microembolism-induced renal failure in rat. Am J Pathol. 2001; 158:75–85. [PubMed: 11141481]
21. Kimura M, Asano M, Abe K, et al. Role of atrophic changes in proximal tubular cells in the peritubular deposition of type IV collagen in a rat renal ablation model. Nephrol Dial Transplant. 2005; 20:1559–1565. [PubMed: 15870225]
22. Lin SL, Kisseleva T, Brenner DA, et al. Pericytes and perivascular fibroblasts are the primary source of collagen-producing cells in obstructive fibrosis of the kidney. Am J Pathol. 2008; 173:1617–1627. [PubMed: 19008372]
23. Grgic I, Duffield JS, Humphreys BD. The origin of interstitial myofibroblasts in chronic kidney disease. Pediatr Nephrol. 2011
24. Humphreys BD, Lin SL, Kobayashi A, et al. Fate tracing reveals the pericyte and not epithelial origin of myofibroblasts in kidney fibrosis. Am J Pathol. 2010; 176:85–97. [PubMed: 20008127]
25. de Borst MH, Prakash J, Sandovici M, et al. c-Jun NH2-terminal kinase is crucially involved in renal tubulo-interstitial inflammation. J Pharmacol Exp Ther. 2009; 331:896–905. [PubMed: 19717791]
26. Lin SL, Chang FC, Schrimpf C, et al. Targeting endothelium-pericyte cross talk by inhibiting VEGF receptor signaling attenuates kidney microvascular rarefaction and fibrosis. Am J Pathol. 2011; 178:911–923. [PubMed: 21281822]
27. Matsui K, Kamijo-Ikemori A, Hara M, et al. Clinical significance of tubular and podocyte biomarkers in acute kidney injury. Clin Exp Nephrol. 2011; 15:220–225. [PubMed: 21153750]
28. Chevalier RL, Forbes MS. Generation and evolution of atubular glomeruli in the progression of renal disorders. J Am Soc Nephrol. 2008; 19:197–206. [PubMed: 18199796]
29. Vaidya VS, Niewczas MA, Ficociello LH, et al. Regression of microalbuminuria in type 1 diabetes is associated with lower levels of urinary tubular injury biomarkers, kidney injury molecule-1, and N-acetyl-beta-D-glucosaminidase. Kidney Int. 2011; 79:464–470. [PubMed: 20980978]

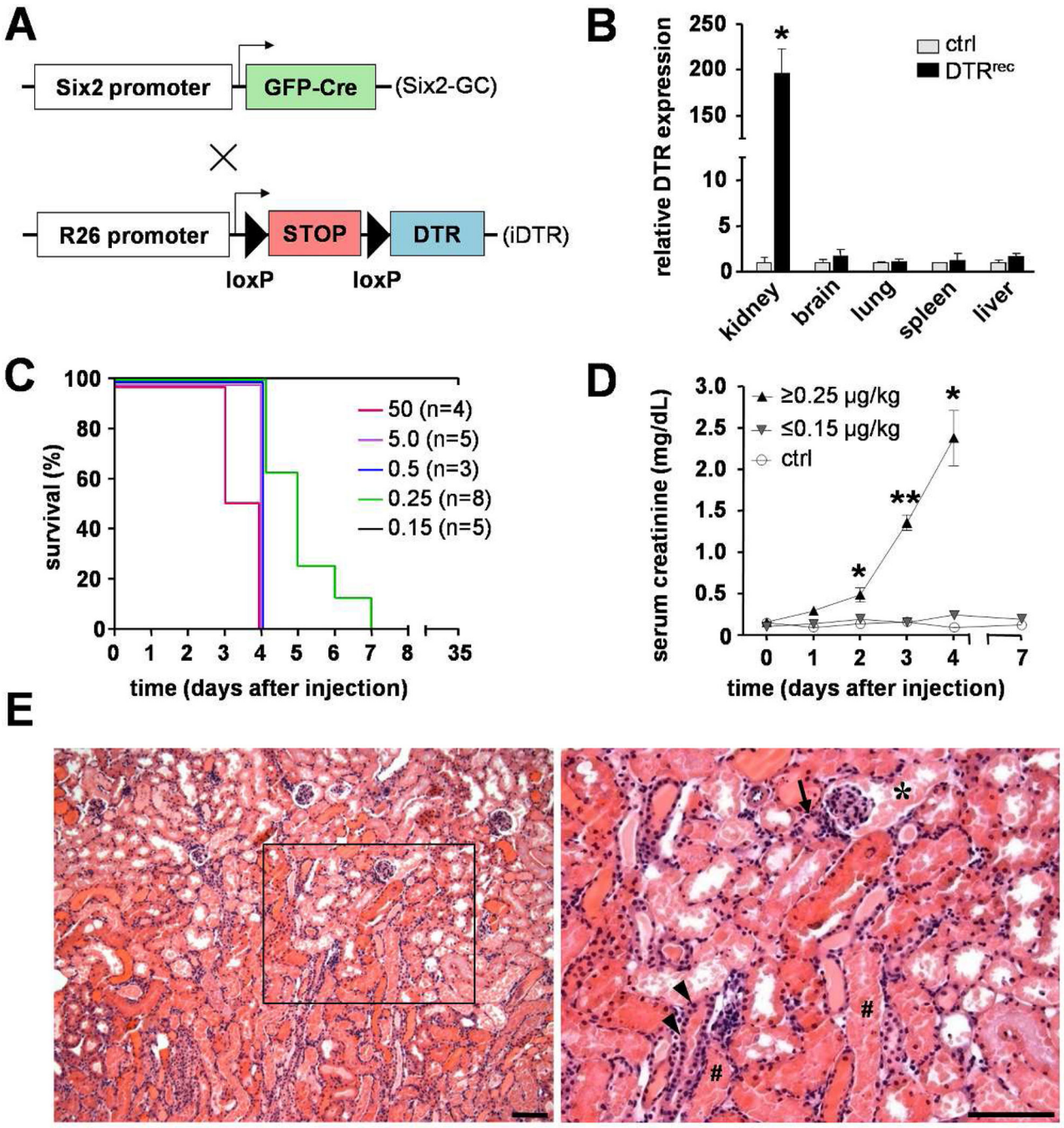

Figure 1. Genetic approach rendering renal epithelial cells susceptible to diphtheria toxin (DT) and DT-induced AKI and survival in DTR^{rec} mice

(A) In bigenic DTR^{rec} mice, GFPCre expression is activated in Six2^{+} renal progenitor cells leading to excision of the loxP-STOP-loxP cassette and heritable induction of the simian diphtheria toxin receptor (DTR). (B) RT-PCR analysis demonstrates kidney-specific induction of DTR expression; n=3–4 for each data point; *P<0.01 vs. control. (C) Kaplan-Meier plot showing survival of DTR^{rec} mice in relation to single DT dose. Doses ≤ 0.15 µg/kg bodyweight allow survival (P=0.001 [log-rank test for trend], P=0.014 [log-rank

(Mantel-Cox) test]). (D) Serum creatinine as a function of time after DT administration; n=2–11 for each data point; *P<0.005, **P<0.0001. (E) Micrographs of an H&E stained DTR^{rec} kidney section 3 days after DT (5μg/kg) injection at two different magnifications. Scale bars: 100μm; (*****) proximal convoluted tubule, (#) straight portion of proximal tubule, *(arrow)* distal tubule, *(arrow heads)* collecting duct.

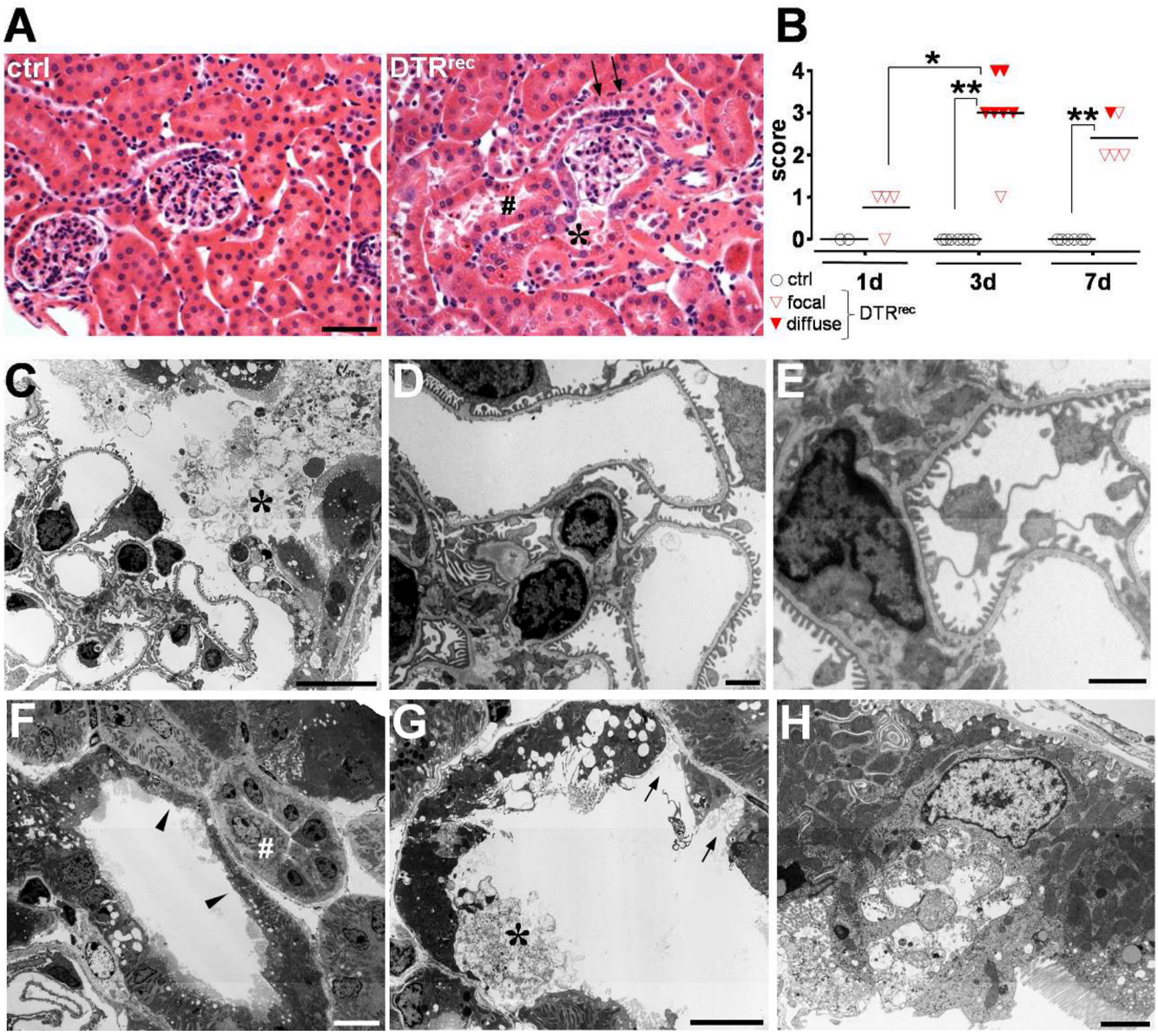

Figure 2. Sublethal DT dose confines acute tubular injury to segments S1/S2

(A) Representative micrographs of H&E stained kidney sections from DTR^{rec} and littermate control 3 days after administration of 0.15μg/kg DT. Signs of acute epithelial cell injury are seen in DTR^{rec} at the tubular pole, contiguous proximal tubule (S1 segment, *) and adjacent convoluted proximal tubules (S2 segment, #). Glomerular tuft, arteriole at the vascular pole and distal tubule (*arrows*) with macula densa appear normal. Scale bar: 50μm. (B) Scoring of acute tubular injury. Focal damage was defined as involvement of less than 50% and diffuse damage as involvement of 50% or more proximal tubules by acute tubular injury. Data points represent individual animals, horizontal lines represent mean values; *P<0.005, **P<0.00001. (C–G) Electron microscopy demonstrates selective injury of the proximal tubular epithelium with vacuolization and swelling of the cytoplasm, loss of brush border (F, *arrow heads*), luminal distension, attenuated epithelial lining, exposed tubular basement

membrane (G, *arrows*), and cellular disruption, detachment (C&G, *asterisks*) and debris. By contrast, endothelial, mesangial and visceral epithelial (podocytes) cells of the glomerular tuft, intercalated (F, #) and principal cells of collecting duct, and interstitial cells show normal cellular details. Scale bars: 10μm. (H) This EM micrograph shows a single damaged proximal tubule epithelial cell captured in the process of disintegration. Of note, flanking epithelial cells appear unaffected (normal mitochondria, preserved brush border), underlining the concept of “toxin receptor mediated cell knockout” on a single cell level in this injury model. Scale bar: 2μm.

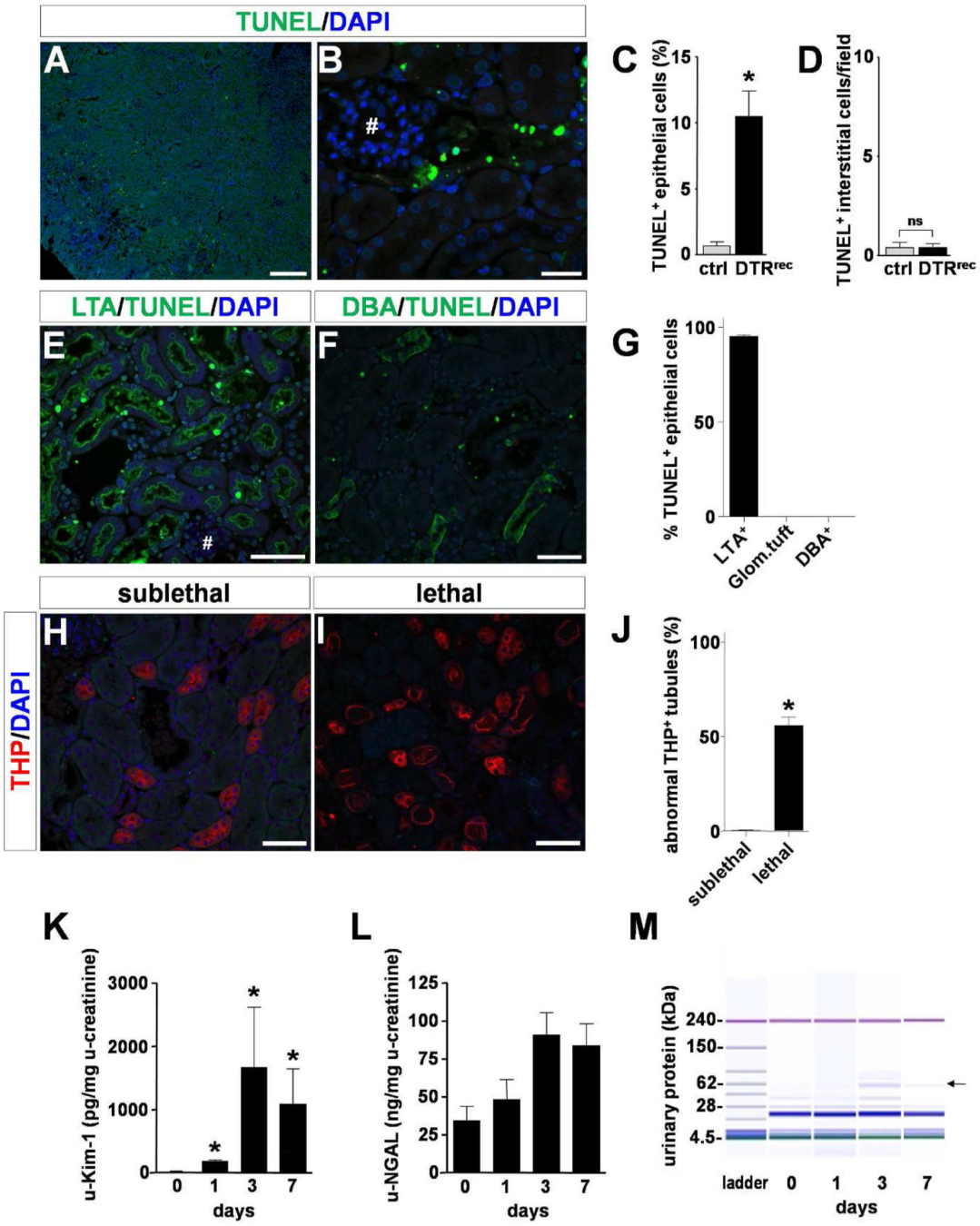

Figure 3. Selective induction of apoptosis in proximal tubule epithelium by sublethal dose of DT

(A–D) TUNEL labeling shows robust and specific DT-mediated induction of apoptosis in tubules of kidney cortex. Representative micrographs are shown at low (A, scale bar: 250μm) and high (B, scale bar: 25μm; # glomerular tuft) magnification. Quantitative analysis is presented in C and D; n=3–5 for each data point; **P*<0.001. (E–G) Segment specific staining and quantification reveals that the vast majority of apoptotic epithelial cells (nuclear staining) are located in LTA^+ proximal tubules (apical staining) and not found in glomerular tufts (#) or DBA^+ collecting ducts (basolateral staining). Scale bars: 50μm, n=5

(*see also* Fig.S3). (H–J) Anti-Tamm Horsfall Protein (THP)/uromodulin immunostained sections show normal overall morphology of thick ascending limbs (TAL) in kidneys from sublethally DT-injured DTR^{rec} animals (0.15μg/kg). By contrast, a large fraction of TAL segments shows overt morphological changes (flattening, cell sloughing) after administration of a lethal DT dose (0.25μg/kg) Scale bars: 50μm, n=4 per group; **P<0.0001*. (K&L) Urinary Kim-1 and NGAL in DTR^{rec} mice after DT (0.15μg/kg) injection; n=4–15 for each data point; **P*<0.05. (M) Urinary protein analysis by chip-based capillary electrophoresis. Representative gel demonstrates transient appearance of higher molecular weight protein signal *(arrow)* consistent with albumin.

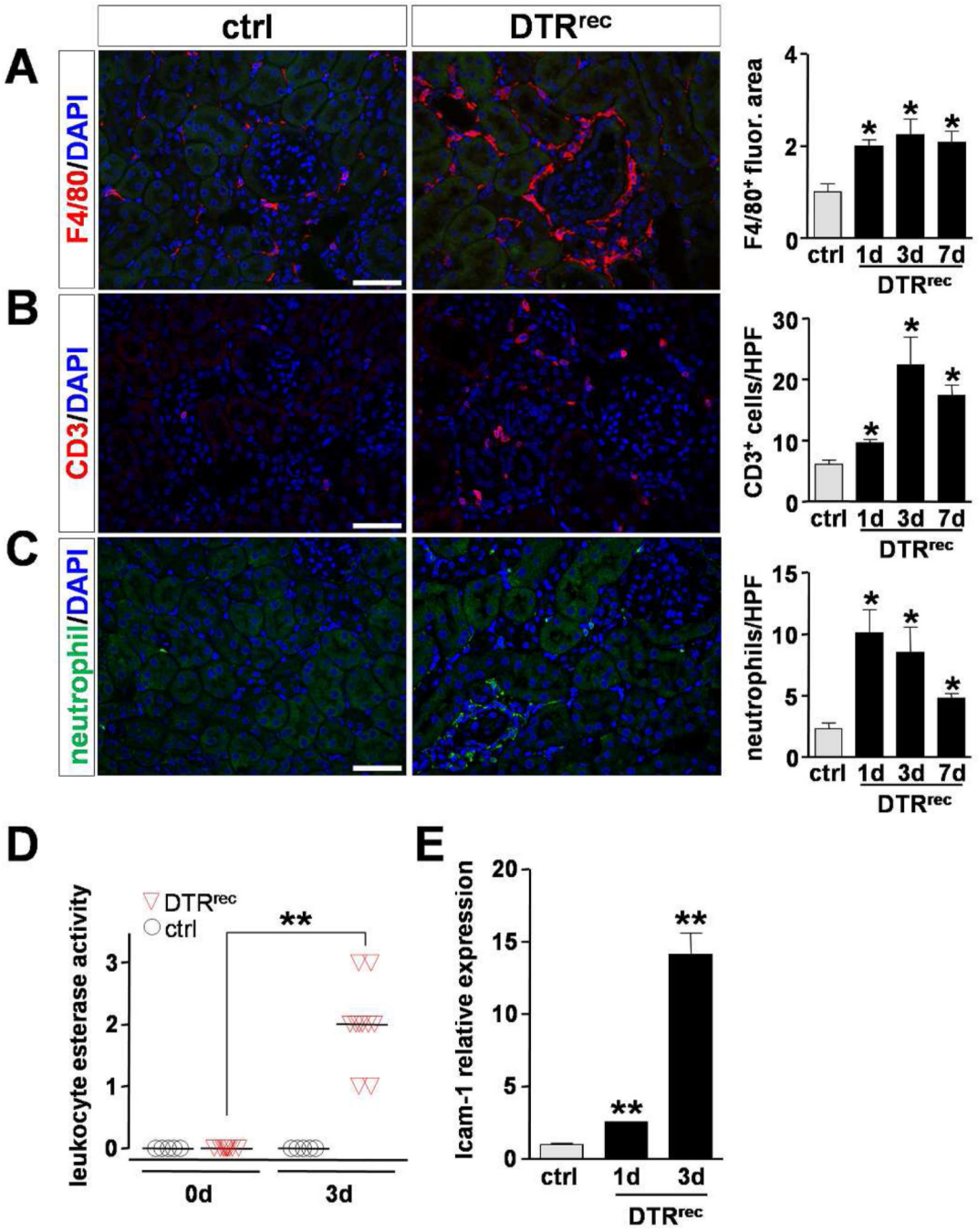

Figure 4. Targeted injury of proximal renal epithelium is followed by mild to moderate inflammatory response

(A–C) Analysis of inflammatory cell populations in kidney sections after DT administration. *Left*: Representative micrographs of immunostained kidney sections detecting macrophages (anti-F4/80), T cells (anti-CD3) and neutrophils (anti-neutrophil), respectively, 3 days after DT injection. Scale bars: 50μm. *Right*: Quantification of immunostained kidney sections. Fluorescence area was normalized to control; n=3–4 for each data point; **P*<0.05 vs control. (D) Reagent strip-based estimate of urinary leukocyte esterase activity [1, small, 2,

moderate, 3, large]. Data points represent individual animals, horizontal lines represent mean values; ***P*<0.00001. (E) Quantitative RT-PCR analysis shows upregulation of ICAM-1 expression in kidneys subsequent to DT-induced epithelial injury; n=3–5 for each data point; ***P*<0.001 vs control.

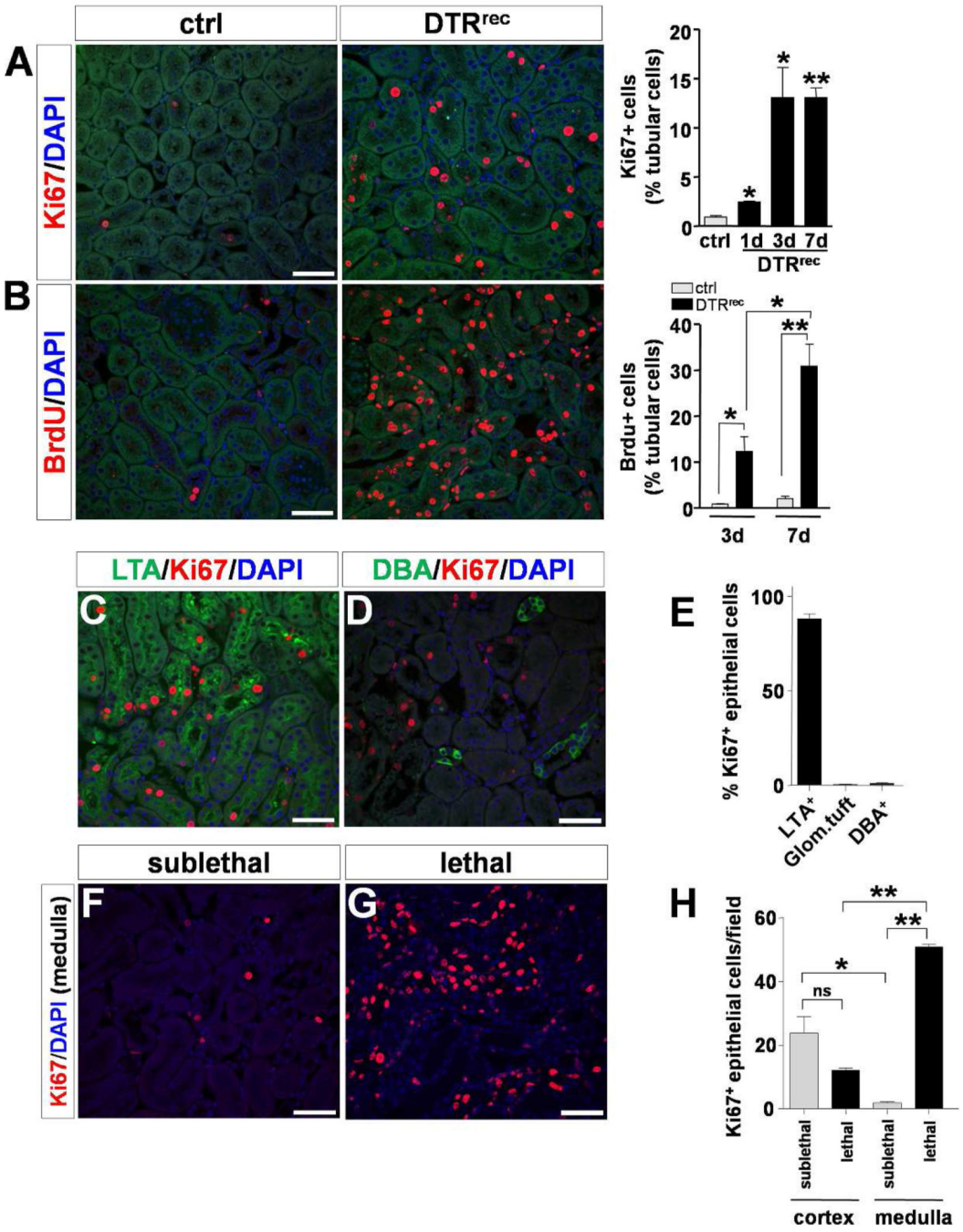

Figure 5. Regenerative response after acute DT-mediated injury to renal epithelium

(A) Cross sectional analysis of actively proliferating cells by anti-Ki67 staining. *Left*: Representative micrographs of kidney sections 3 days after DT exposure. Scale bar: 50μm. *Right*: Quantification of $Ki67^+$ cells in kidney sections; n=3–5 for each data point; **P*<0.05, ***P*<0.001 vs control. (B) Longitudinal proliferation assay by BrdU pulsing and labeling. *Left*: Representative micrographs of anti-BrdU immunostained kidney sections at day 7 after DT. Scale bar: 50μm. *Right*: Quantification of $BrdU^+$ cells in kidney sections; n=3–5 for each data point; **P*<0.05, ***P*<0.005. (C–E) Segment specific staining and quantification

reveals that the majority of proliferating epithelial cells are located in LTA^+ proximal tubules 3 days after administration of a sublethal DT dose. Scale bars: 50μm (*see also* Fig.S5). (F–H) In sublethally injured DTR^{rec} kidneys the general prevalence of $Ki67^+$ epithelial cells is higher in cortex than in medulla. Lethal DT doses lead to a reversal of this ratio mirroring the increased severity of damage to proximal tubules with fewer cells left to proliferate. Scale bars: 50μm, n=4–6 per group; **P*<0.01, ***P*<0.0001.

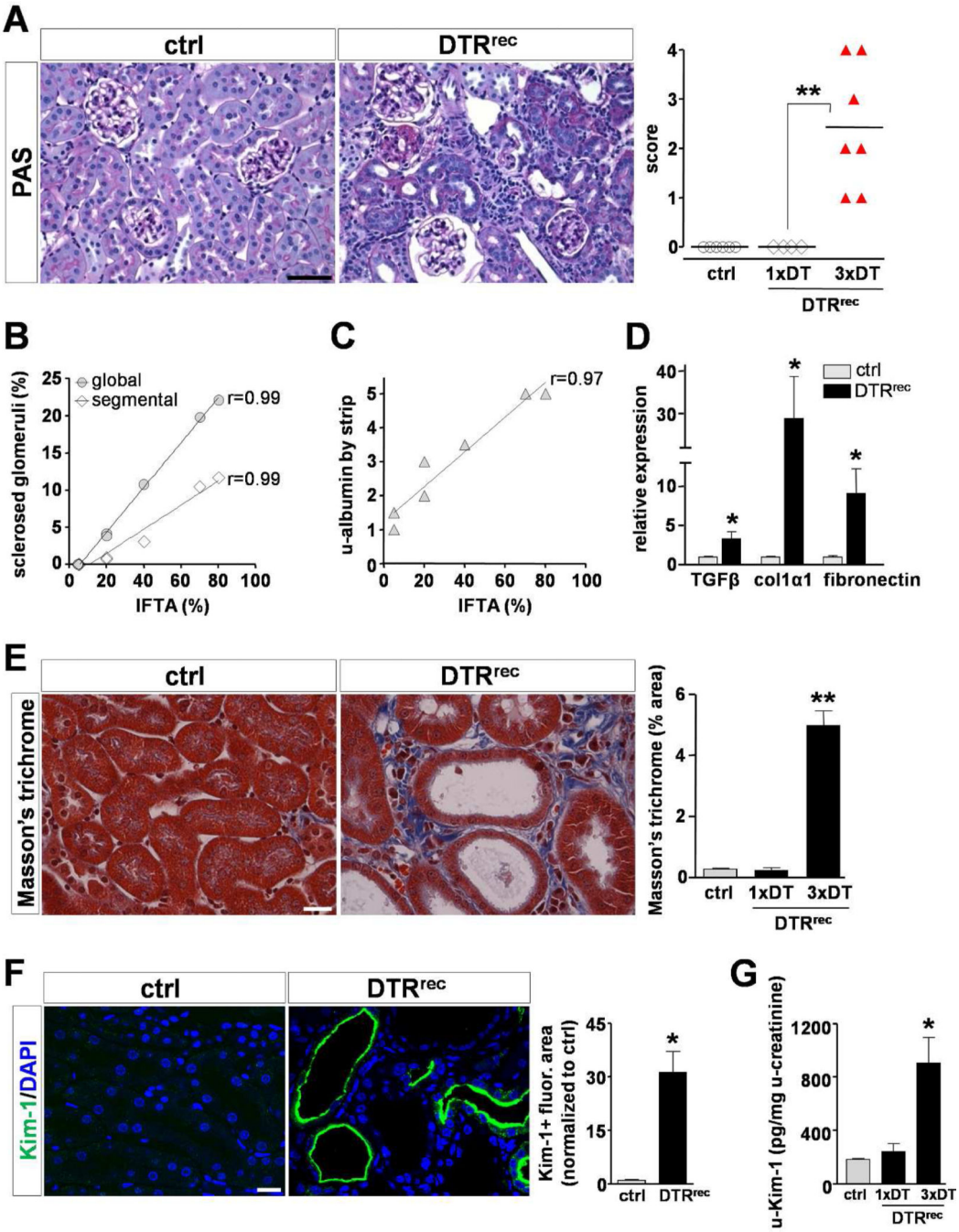

Figure 6. Repeated injury to proximal tubular segments S1/S2 leads to development of tubulointerstitial fibrosis with secondary glomerulosclerosis

(A) *Left*: Representative micrographs of PAS stained kidney sections. Repeatedly injured DTR^{rec} kidney shows signs of chronic tubulointerstitial injury including atrophic tubules and expanded tubulointerstitium. Scale bar: 50μm. *Right*: Scoring of chronic tubulointerstitial damage. Data points represent individual animals, horizontal lines represent mean values; $^{**}P<0.005$. (B) Positive correlation between % interstitial fibrosis/ tubular atrophy (IFTA) and number of globally or segmentally sclerosed glomeruli in these

kidneys. Data points represent measurements of individual animals (n=7), lines represent best fits. (C) Positive correlation between % IFTA and albuminuria in these mice. (D) Quantitative RT-PCR analysis shows upregulation of TGFβ1, collagen 1α1 and fibronectin mRNA levels in repeatedly DT-injured kidneys; **P*<0.05. (E) Assessment of extracellular matrix (ECM) deposition by Masson's trichrome staining. *Left*: Representative micrographs of Masson's trichrome stained kidney sections. Scale bar: 20μm. *Right*: Quantification of kidney area positive for ECM relative to total area; n=4–5 for each data point; **P*<0.0001. (F) Staining of kidney sections with Kim-1-specific antibody. *Left:* Representative micrographs reveal pronounced expression of Kim-1 in tubules of fibrotic DTR^{rec} kidneys after repeated DT treatment. Note abnormally dilated tubules and apical localization of Kim-1. Scale bar: 20μm. *Right*: Semi-automated quantitative analysis of Kim-1^{+} fluorescence area normalized to control. Values are shown as mean ± SEM, n=3–5 for each data point; **P*<0.01. (G) ELISA-based quantification of Kim-1 in urine after single (1×) or repeated (3×) DT injection (0.15μg/kg). Consistent with Kim-1 staining, urinary Kim-1 was significantly higher in repeatedly injected DTR^{rec} mice compared to littermate controls. By contrast, DTR^{rec} animals with single DT exposure showed values comparable to those of control animals at 5 weeks. Data are given as mean ± SEM, n=3–5 for each data point; **P*<0.05 vs. control.

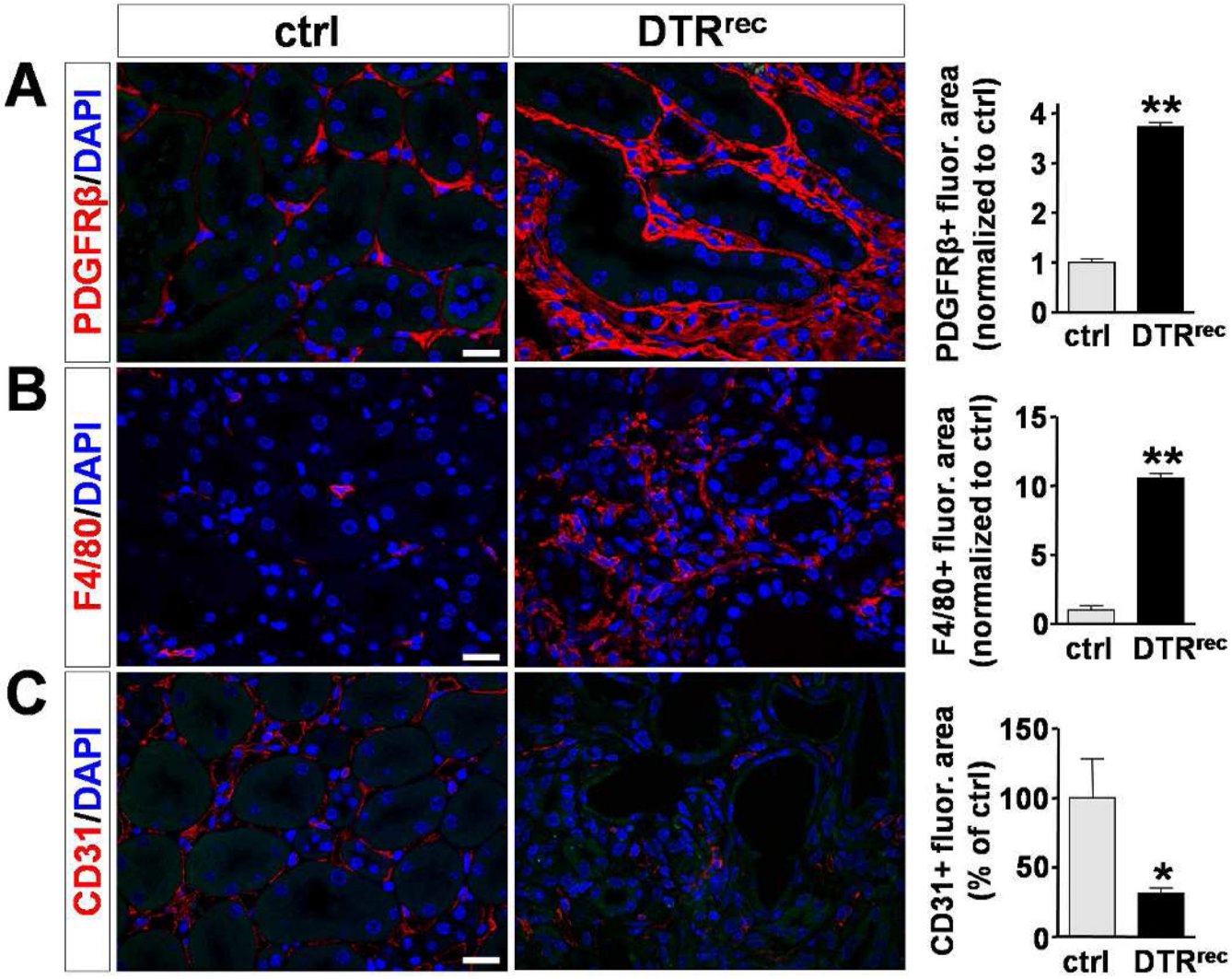

Figure 7. Repeatedly injured DTR^{rec} kidneys exhibit expansion of pericytes/perivascular fibroblasts and macrophages but decrease in capillary density

Immunostaining for specific cell markers and quantification. *Left:* Representative micrographs of kidney sections from repeatedly (3×) DT-treated (0.15μg/kg) DTR^{rec} and control animals stained for PDGFRβ (pericytes/perivascular fibroblasts), F4/80 (macrophages) and CD31 (endothelial cells). Scale bars: 20μm. *Right:* Quantification of fluorescence area stained positive for PDGFRβ, F4/80 and CD31; n=3–5 for each data point; **P*<0.05, ***P*<0.0001.